

Article

The Critical Depth of Freeze-Thaw Soil under Different Types of Snow Cover

Qiang Fu *, Renjie Hou, Tianxiao Li, Peiru Yan and Ziao Ma

School of Water Conservancy & Civil Engineering, Northeast Agricultural University, Harbin 150030, China; hourenjie888@126.com (R.H.); litianxiao@neau.edu.cn (T.L.); ypr18846920256@126.com (P.Y.); maziao@hotmail.com (Z.M.)

* Correspondence: fuqiang0629@126.com; Tel.: +86-0451-5519-0209 or +86-0451-5519-1164

Academic Editor: Xixi Wang

Received: 17 February 2017; Accepted: 22 May 2017; Published: 25 May 2017

Abstract: Snow cover is the most common upper boundary condition influencing the soil freeze-thaw process in the black soil farming area of northern China. Snow is a porous dielectric cover, and its unique physical properties affect the soil moisture diffusion, heat conduction, freezing rate and other variables. To understand the spatial distribution of the soil water-heat and the variable characteristics of the critical depth of the soil water and heat, we used field data to analyze the freezing rate of soil and the extent of variation in soil water-heat in a unit soil layer under bare land (BL), natural snow (NS), compacted snow (CS) and thick snow (TS) treatments. The critical depth of the soil water and heat activity under different snow covers were determined based on the results of the analysis, and the variation fitting curve of the difference sequences on the soil temperature and water content between different soil layers and the surface 5-cm soil layer were used to verify the critical depth. The results were as follows: snow cover slowed the rate of soil freezing, and the soil freezing rate under the NS, CS and TS treatments decreased by 0.099 cm/day, 0.147 cm/day and 0.307 cm/day, respectively, compared with that under BL. In addition, the soil thawing time was delayed, and the effect was more significant with increased snow cover. During freeze-thaw cycles, the extent of variation in the water and heat time series in the shallow soil was relatively large, while there was less variation in the deep layer. There was a critical stratum in the vertical surface during hydrothermal migration, wherein the critical depth of soil water and heat change gradually increased with increasing snow cover. The variance in differences between the surface layer and both the soil water and heat in the different layers exhibited “steady-rising-steady” behavior, and the inflection point of the curve is the critical depth of soil freezing and thawing. This critical layer is a demarcation point between frozen soil and non-frozen soil, delineating the boundary between soil water and heat migration and non-migration. Furthermore, with increasing snow cover thickness and increasing density, the critical depth gradually increased.

Keywords: freezing and thawing soil; soil water-heat transfer; hydrothermal variation; time series

1. Introduction

Soil is a multiphase system composed of solids, liquids and gas. Material, energy and information are exchanged between the soil and the environment during the atmospheric cycles in a seasonally frozen soil region [1]. Climate is an important natural factor influencing hydrothermal transport in soils, and it affects the spatial and temporal distribution and variation of soil water and heat [2–4]. The freeze-thaw cycle in soil is a complicated process involving physical, chemical and mechanical principles of action accompanied by heat conduction [5], water phase transition [6] and solute migration [7]. The freezing and thawing layer in the soil includes the lower boundary of the cold-influenced environment, and its variation changes the spatial distribution of soil water and heat,

which affects the living environment for vegetation. Soil salinity moves upwards with liquid water driven by temperature gradients, and a large amount of water loss is induced by evaporation, leading to increasing soil salinization [8–10]. Therefore, changes in the active layer thickness in permafrost regions and in the soil water-heat transfer affect hydrological and terrestrial ecosystems [11] and physical and geochemical processes [12,13]. These changes affect crop survival [14] and influence the scientific implementation of agricultural irrigation.

The freezing and thawing of soils are the result of complex influences from meteorological and environmental conditions on the surface water heat, and soil water phase changes reduce the soil permeability, thus affecting the soil hydraulic properties and erosion resistance [15]. In permafrost regions, the soil freezing layer can significantly reduce the snowmelt seepage and increase the spring snowmelt runoff [16]. Research on energy exchange and water cycles in the process of soil freeze-thaw cycles has been conducted by many scholars [17,18]. Kurylyk [19] studied the different forms of the Clapeyron equation and the relationship between the soil-water characteristic curve and the freezing curve, which laid the foundation for establishing a freeze curve and a water conduction model for unsaturated freeze-thaw soil. Xiang [20] established a water-heat coupled model on the basis of the physical process of hydrothermal equilibrium, and snow and soil data from a typical test site in northeastern Sanjiangyuan were used to validate the model. The results indicated that the changes in soil water content, soil temperature and freezing depth were dependent on the ambient air temperature and the snow cover conditions. The temporal and spatial variation of soil water content is more complicated than temperature in water and heat transfers. The freezing of soils hinders the evaporation of water to a certain extent; soil freezing and thawing caused by an abrupt increase or decrease in the ambient temperature can also influence the ecology of an area [21].

The movement of the critical layer is related to the hydrothermal characteristics of the soil and the exchange of water energy between the land surface and the atmosphere. Therefore, an increasing number of frozen soil test studies have focused on the critical layer. Nelson [22] proposed that the increase of the critical depth of seasonal frozen-thawing soil will lead to the increase of ground subsidence, which will affect the normal operations of oil pipelines and related facilities in cold areas. Ge [23,24] used the groundwater flow model (MODFLOW) and Saturated-Unsaturated Transport model (SUTRA) under several assumptions to simulate the hydrothermal conditions of surface soils in the Qinghai-Tibet railway area, predicting the trend of thickness variation of permafrost in the Qinghai-Tibet Plateau. Shiklomanov [25] used the Stefan method for high-precision mapping in the Alaskan Kuparuk watershed in the United States, and in the calculation process, the freezing index was used to characterize the effect of climate change on the thickness of the frozen layer. Liu [26], based on the average surface temperature and soil parameters of permafrost regions, used the simple algorithm for soil freezing and thawing depth (X-G algorithm) to simulate the freezing and thawing process of permafrost in the Maanshan Mountains and analyzed the factors that influence the thickness of the active layer. Zhang [27] calibrated and verified the dynamic simulation model of soil water and heat (COUPMODEL) using monitoring data from the Qinghai-Tibet Plateau, suggesting that organic matter has low thermal conductivity and high heat capacity. These characteristics reduced the influence of soil thermal conditions on solar radiation. Chang [28] found that there was a significant Boltzmann function between the ground temperature and the water level in the active layer of permafrost. The change of surface cover and climate change will lead to changing hydraulic relationships between groundwater and river water, which will cause changes throughout the entire hydrological process. Previous studies have focused on analyzing water and heat transfer through dynamic simulations of frozen soils. However, those studies lack a definition of the critical level of soil water and heat transfer. In this study, we explored the critical depth of soil water and heat transfer under different snow cover conditions, and comparatively analyzed the influence of different treatments on the position of the critical level.

To determine the mechanisms underlying soil water and heat transfer, the dynamic pattern and spatial distribution of soil water and heat in the black soil area of Songnen Plain, northeastern China, were studied. The critical depth of the soil water-heat transfer is defined under different snow

Table 1. Soil physical properties.

Soil Depth (cm)	Bare Land		Natural Snow		Compacted Snow		Thick Snow	
	Field Capacity (%)	Soil Dry Density ($\text{g}\cdot\text{cm}^{-3}$)	Field Capacity (%)	Soil Dry Density ($\text{g}\cdot\text{cm}^{-3}$)	Field Capacity (%)	Soil Dry Density ($\text{g}\cdot\text{cm}^{-3}$)	Field Capacity (%)	Soil Dry Density ($\text{g}\cdot\text{cm}^{-3}$)
5	30.54	1.34	33.46	1.38	34.52	1.39	31.57	1.41
10	30.21	1.25	32.64	1.35	32.51	1.34	29.21	1.42
15	33.21	1.31	32.57	1.42	31.24	1.35	29.36	1.47
20	31.28	1.22	32.18	1.43	33.24	1.32	31.24	1.55
40	32.61	1.32	31.16	1.46	30.71	1.36	28.54	1.57
60	29.46	1.33	29.87	1.49	31.19	1.40	31.24	1.59
100	32.94	1.35	33.61	1.49	32.76	1.57	33.12	1.63
140	31.75	1.48	30.19	1.52	30.91	1.59	32.71	1.59
180	33.21	1.38	32.16	1.54	32.16	1.54	29.54	1.60

2.2. Test Design

The test site was divided into four experimental areas. Each area block was established with a 10×10 m boundary to prevent water migration and diffusion between the different experimental blocks, and a 1-m-deep plastic film water barrier was placed along the borders. In each experimental area, a permafrost measuring instrument (Jinzhou Licheng LQX-DT, Jinzhou, China) was planted and used to determine the change in freezing depth during freezing and thawing. One set of JL-04 soil temperature sensors (Qingshengdianzi, Handan, China) was embedded in each area to measure the soil temperature and water content at soil depths of 5, 10, 15, 20, 40, 60, 100, 140 and 180 cm; the temperature logger was set to automatically read data at 9:00 a.m. daily. Simultaneously, two time-domain reflectometers (TDR) system (IMKO, Ettlingen, Germany) were established in each test area to compare the soil moisture content (measured as liquid moisture content) with the data extracted by the sensor to ensure its accuracy. A meteorological environment monitoring system (Jinzhou Yangguang, Jinzhou, China) was set up in the open area near the test site, and the meteorological indexes such as the ambient temperature, dew point temperature, evaporation, total radiation and net radiation were automatically recorded.

During the experiment, four experimental areas were established as follows: natural snow (NS), compacted snow (CS), thick snow (TS) and bare land (BL). Among these areas, the BL treatment was maintained with artificial snow removal. The NS area retained the original snow without disturbance; the snow cover thickness stability was 15 cm, and the snow density was 0.137 g/cm^3 . The CS area was simulated with artificial snow, and a constant-quality polyethylene plate was used (density = 9.8 kg/cm^2 , specifications $2.5 \text{ m} \times 1.5 \text{ m}$) to compact it, ensuring that the snow density was uniform; the snow thickness was 15 cm, and the density was 0.212 g/cm^3 . The TS area was simulated with artificial snow to ensure that the snow cover was consistent with the state of natural snow; the thickness of snow cover was 30 cm, and the snow density was 0.140 g/cm^3 .

During the experiment, the snow density and liquid water content were measured with a Snow Fork Snow Characteristic Analyzer (Helsinki University, Helsinki, Finland). The snow temperature was measured with a probe thermometer. The thickness of the snow was measured daily with a steel ruler. The physical characteristics of snow indicators are shown in in Table 2.

Table 2. Physical parameters of snow cover.

Treatment Method	Initial Freezing Period (15 December 2014)			Freezing Stability Period (30 January 2015)			Thawing Period (15 March 2015)		
	Snow Temperature ($^{\circ}\text{C}$)	Snow Water Content (%)	Snow Density (g/cm^3)	Snow Temperature ($^{\circ}\text{C}$)	Snow Water Content (%)	Snow Density (g/cm^3)	Snow Temperature ($^{\circ}\text{C}$)	Snow Water Content (%)	Snow Density (g/cm^3)
Natural snow	−8.9	18.6	0.118	−12.9	24.2	0.137	−7.8	28.6	0.110
Compacted snow	−9.5	26.4	0.174	−11.3	36.5	0.212	−6.3	38.3	0.189
Thick snow	−8.8	20.3	0.122	−10.5	25.0	0.140	−5.9	27.1	0.117

During the test, the three different snow-covered areas were artificially processed after each snowfall. From Figure 2 we can see that the snow parameters in the areas tended to be stable during 15 December 2014–1 March 2015. The snow thickness was approximately 30 cm in the TS plot and fluctuated around 15 cm in the NS and CS plots. The Figure 3 showed that the trends of the daily average temperature and daily total radiation value followed similar patterns, showing initial decreases followed by increases. The lowest daily average temperature of $-23.11\text{ }^{\circ}\text{C}$ appeared on 13 January 2015, and the minimum value of the total accumulated daily radiation of 0.23 MJ/m^2 appeared on 20 December 2014.

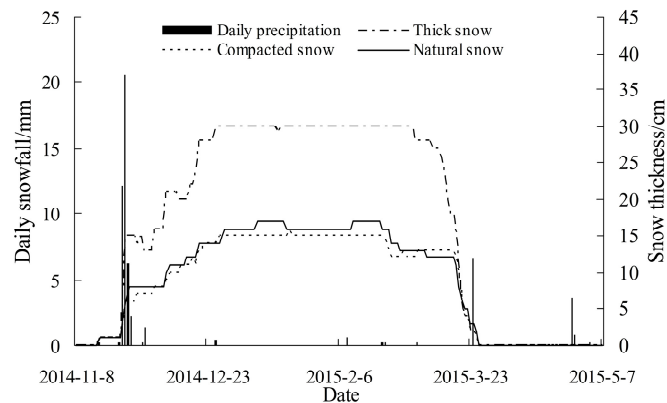


Figure 2. Snow amount and thickness variation in the test period.

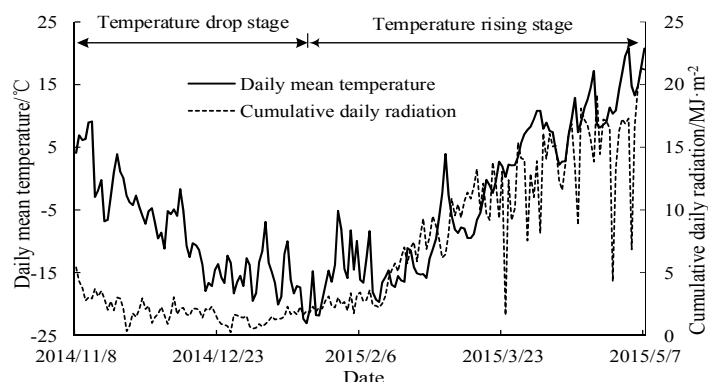


Figure 3. Daily average temperature and daily total radiation variation in the test period.

2.3. Analytical Methods

2.3.1. Data Processing

During the data analysis, we combined the freezing depth, soil moisture content and temperature data with the meteorological indicators and snow characteristic parameters. Moreover, we plotted the spatial distribution of the soil temperature and liquid water content under different snow cover treatments using Sigmaplot software v. 12.5 (SYSTAT, Richmond, CA, USA). Next, we analyzed the variability of the soil water content and temperature along the vertical profile under different snow cover treatments. We used SPSS software v. 13.0 (IBM, Amon, NY, USA) to analyze the variation coefficient and variance of the soil temperature and water content.

2.3.2. Evaluation Indicators

(1) Standard deviation:

The standard deviation reflects the distance of the data from the mean of the combined elements, and the standard deviation of time series x_i of soil parameters in any soil layer can be expressed as follows:

$$\sigma = \sqrt{\sum_{i=1}^N (x_i - \mu)^2 / (N - 1)} \quad (1)$$

$$\mu = \frac{1}{N} \sum_{i=1}^N x_i \quad (2)$$

where N is the sample number; μ is the sample mean; and $i = 1, 2, 3 \dots N$.

(2) Variance:

The variance is the average of the sum of the squared deviations of each data point and their arithmetic mean; usually expressed in σ^2 , it is typically used to measure the degree of difference of statistical data:

$$D = \sigma^2$$

(3) Variation coefficient:

In this study, the coefficient of variation, C_v , reflects the relative variability, which mainly reflects the degree of time series dispersion in the temperature and liquid water temperature, as follows [29]:

$$C_v = \frac{\sigma}{|\mu|} \times 100\% \quad (3)$$

According to the size of the variation coefficient, the degree of variation in the soil temperature and liquid water content can be divided into three categories: weak variation ($C_v \leq 10\%$), medium variation ($10\% < C_v < 100\%$) and high variation ($C_v \geq 100\%$) [30].

As the measurement depths of the soil temperature and moisture were 5, 10, 15, 20, 40, 60, 100, 140 and 180 cm in the original text, the range of the soil temperature and moisture in a unit soil layer between 5 and 10 cm was calculated as the maximum value of the 10-cm soil layer minus the minimum value of the 5-cm soil layer, and the value was divided by 5 cm (10–5 cm). According to this method, the change range of the soil moisture and temperature in a unit soil layer was calculated for depths of 10–15 cm, 15–20 cm, 20–40 cm, etc. For the variance of a unit soil layer, the variance of the soil temperature and water time series in the 5-cm and 10-cm soil layers were obtained, and the difference value between the two was divided by 5 cm (10–5 cm); in the same way, the variances of the unit soil layers at depths of 10–15 cm, 15–20 cm, 20–40 cm, 40–60 cm, 60–100 cm, 100–140 cm and 140–180 cm were obtained sequentially. Finally, the standard deviation of the temperature and moisture of the unit soil layer was divided by the average temperature and moisture content of the soil layer in the area and the variation coefficient of the temperature and moisture in the unit soil layer can be obtained.

3. Results and Analysis

3.1. The Process of the Soil Freezing Depth Curve

The measurement cycle of the experiment followed a soil freeze-thaw cycle (8 November 2014–7 May 2015). At the onset of freezing, the soil was presented in a one-way frozen state from the top to the bottom, whereas in the melting period, the frozen soil area showed a “two-way” melting state. There were differences in the freezing process of the soil due to the different snow cover conditions.

These differences affected the critical depth of soil freezing. The soil freezing process curve is shown in Figure 4.

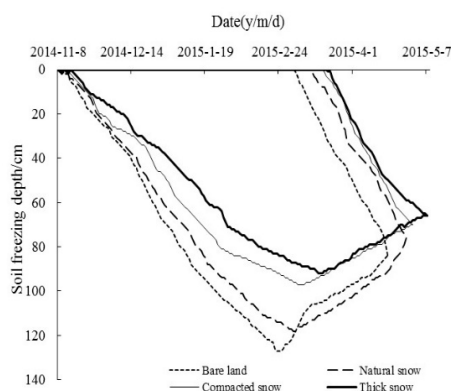


Figure 4. The soil freezing process curve.

An analysis of the overall trends showed that the surface soil was the first to melt under BL conditions on 25 February 2015. Increases in the ambient temperature resulted in snow melt, and under NS, TS and CS conditions, the soil presented a phenomenon of melting in turn. The analysis showed that the maximum freeze depth was 127 cm under the BL treatment, whereas under the NS, CS and TS treatments, the maximum freeze depths were 118 cm, 95 cm and 86 cm, respectively. Under normal circumstances, with the increase of the snow density, the thermal conductivity of the snow cover is enhanced under the CS treatment, and the change in the atmospheric temperature is more likely to affect the heat transfer of the soil, thereby increasing the freezing depth. However, in this study, the data in Table 2 showed that in the CS treatment, the liquid water content of the snow was greater than that of the NS treatment, and the heat capacity of water ($4.2 \times 10^3 \text{ J}/(\text{kg}\cdot^\circ\text{C})$) was greater than the heat capacity of snow ($2.1 \times 10^3 \text{ J}/(\text{kg}\cdot^\circ\text{C})$). The liquid water in snow absorbs more energy, which hinders the dissipation of soil heat. Therefore, the soil freezing depth under the CS treatment was less than that of the NS treatment.

Snow cover prolonged the soil freezing time. Under the BL treatment, the soil complete thaw date was 19 April. The time at which the soil completely thawed under the NS, CS and TS treatments exhibited increases of 9, 12 and 17 days, respectively, compared with BL. Furthermore, the change trend of the soil freeze depth curve exhibited changes in the slope that were relatively large at the early freeze stage; with the continuation of the freezing process, the slope of the freeze curve changed slowly and tended to become stable within a certain period of time. Similarly, changes in the soil freezing under the NS, CS and TS treatments exhibited decreasing trends, to different extents, compared with the BL treatment. The specific change process of freezing rate is shown in Table 3:

Table 3. The soil freezing rate.

Soil Layer Depth (cm)	Soil Freezing Rate (cm/day)			
	Bare Land	Natural Snow	Compacted Snow	Thick Snow
0–10	0.91	0.71	0.67	0.63
10–20	1.11	1.43	1.43	0.67
20–30	1.25	1.25	1.25	0.91
30–40	1.43	1.43	1.11	0.77
40–50	1.67	1.67	1.43	0.91
50–60	2.00	1.25	1.25	1.25
60–70	1.67	1.11	1.00	1.11
70–80	1.43	1.00	1.11	0.67
80–90	1.11	1.25	0.71	0.40
90–100	1.11	0.91	0.50	0.33
100–110	0.71	0.67	-	-
110–120	0.67	0.45	-	-
120–130	0.45	-	-	-

A comparative analysis of the soil freezing rate indicates that under the BL treatment conditions, the soil freezing rate was 0.91 cm/day in the 0–10-cm soil layer, which is relatively stable. With the continuous migration of the freezing front, the freezing rate rapidly increased in the 10–60-cm soil layer, and the average freezing rate was 1.62 cm/day, especially in the 50–60-cm soil layer, where the freezing rate reached a peak value. The freezing rate showed a gradual weakening trend when the freezing depth reached 110–120 cm, where the freezing rate was only 0.67 cm/day. During the whole freezing period, the freezing rate of the vertical section of soil first increased and then decreased. Under NS conditions, the freezing trend was the same as in the BL treatment; however, in the same soil layer, the freezing rate exhibited a decreasing trend to different extents compared with the BL treatment. Similarly, in the 40–50-cm soil layer, the freezing rate reached 1.67 cm/day, which was the peak freezing rate under these conditions. The freezing rate gradually decreased below 50 cm and finally reached a stable state in the 100–110-cm soil layer. Furthermore, compared with the BL and NS treatments in the same soil layer, the freezing rate decreased under the CS and TS treatments, reaching a steady state at 90–100 cm and 80–90 cm, respectively.

3.2. Soil Temperature Variation

The transfer process of soil temperature under different snow cover conditions determined in the present study is plotted in Figure 5. In addition, the time series of the soil temperature in different soil layers were analyzed with SPSS 19.0; the results are shown in Table 4.

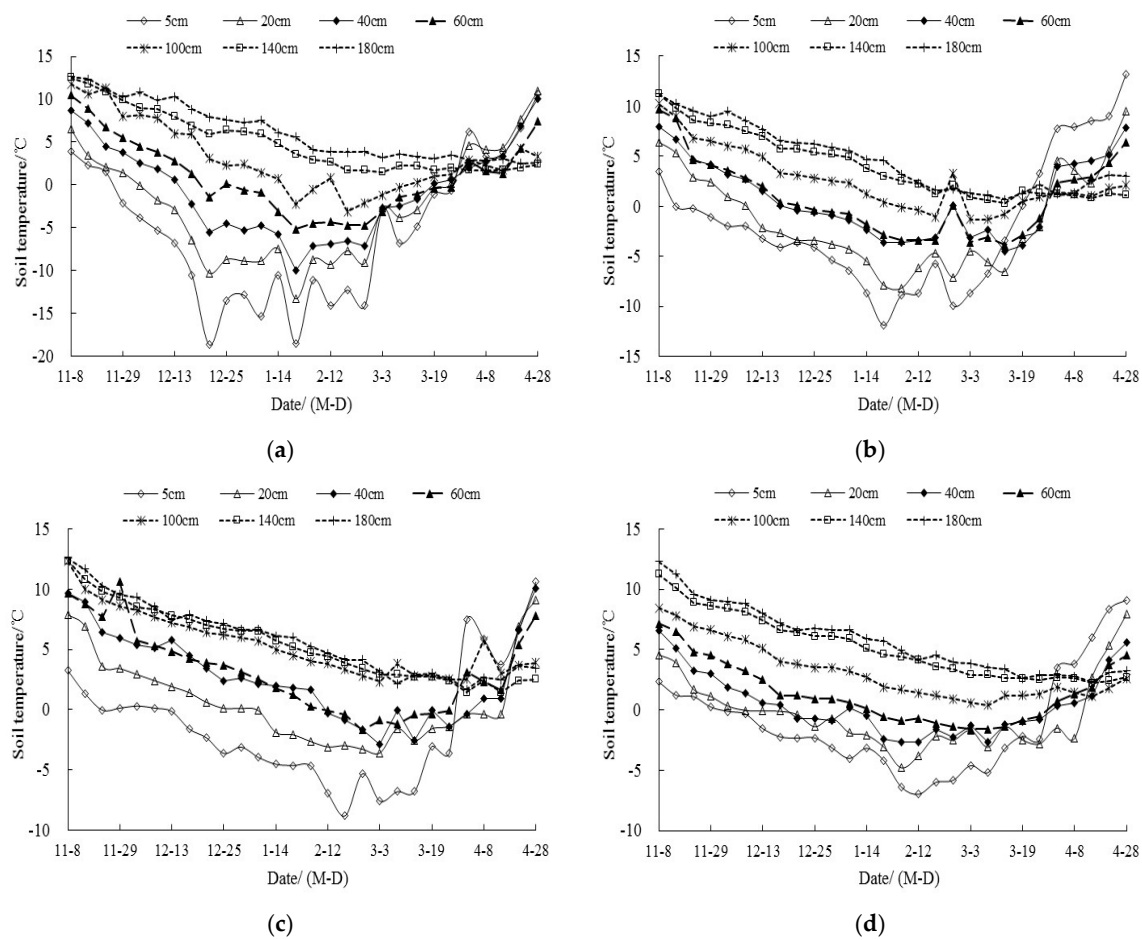


Figure 5. Variation in soil temperature under different snow covers. (a) Bare land; (b) natural snow; (c) compacted snow; (d) thick snow.

Table 4. Analysis of soil temperature variability in unit soil layers under different snow cover treatments.

Soil Depth /cm	Bare Land			Natural Snow			Compacted Snow			Thick Snow		
	<i>R</i> (°C)	<i>C_v</i> (%)	<i>D</i> (°C)									
Δ(10–5)/5	0.65	12.138	0.361	0.64	11.578	0.298	0.63	11.967	0.276	0.59	14.134	0.328
Δ(15–10)/5	0.63	11.142	0.298	0.55	12.127	0.273	0.58	15.647	0.342	0.44	11.197	0.259
Δ(20–15)/5	0.57	9.142	0.218	0.46	11.345	0.256	0.56	8.431	0.224	0.32	7.342	0.238
Δ(40–20)/20	0.36	9.534	0.182	0.35	8.564	0.198	0.53	6.286	0.203	0.29	7.854	0.214
Δ(60–40)/20	0.48	5.782	0.183	0.23	5.335	0.167	0.48	4.973	0.138	0.27	5.342	0.127
Δ(100–60)/40	0.34	4.934	0.158	0.18	3.245	0.137	0.34	2.946	0.131	0.12	2.947	0.111
Δ(140–100)/40	0.20	2.645	0.061	0.13	1.672	0.059	0.20	1.754	0.067	0.13	1.824	0.061
Δ(180–140)/40	0.06	0.891	0.017	0.07	0.624	0.013	0.06	0.534	0.016	0.06	0.542	0.013

Notes: *R* represents the range; *C_v* represents the variation coefficient; *D* represents the variance.

The overall analysis indicated that the soil temperature sequence in the whole freeze-thaw cycle exhibited a trend of decreasing first and then increasing over time. In the soil vertical section, the changes of soil temperature in the 0–40-cm soil layer under different treatment conditions were more significant; this tendency indicates that the temperature change in this region was relatively large, while those between 40 and 100 cm were relatively minor. However, in the 100–180-cm soil layer, the change gradient was small, indicating that the soil temperature of this region was minimally affected by the external environment.

In the BL treatment, the soil temperature ranged from -20.24 to 14.47 °C in the 0–40-cm soil layer, indicating a large variation in temperature. As the soil depth increased, the variation of the soil temperature ranged from -10 to 11.8 °C in the 40–140-cm soil layer, and the extent of the soil temperature change was relatively weak. Meanwhile, the variation range of the soil temperature in the deep 140–180-cm soil layer was 3.2 – 12.7 °C. Thus, the soil temperature changed minimally, and these soils did not freeze.

In the NS treatment area, the soil temperature ranged from -7.55 to 13.15 °C in the 0–40-cm soil layer, and the variation of the soil temperature decreased greatly compared with that under the BL treatment. In addition, the temperature variation ranges between the 40–140-cm and 140–180-cm soil layers were -3.9 – 10.23 °C and 4.7 – 13.8 °C, respectively. In the same soil layer, the range of the soil temperature variation range decreased under the three snow cover treatment conditions compared with the bare soil treatment, and the changes in temperature were minor.

Similarly, under the CS and TS treatments, the soil temperature ranges were -6.82 – 12.55 °C and -5.86 – 12.81 °C, respectively, in the 0–40-cm soil layer. The soil temperature change trend under these two treatments was slower than that under the BL and NS treatments. Furthermore, the soil temperatures in the 40–140-cm and 140–180-cm soil layers gradually became stable with the increasing soil depth. The differences in soil temperature under the four treatments exhibited the following order of extent: BL > NS > CS > TS.

Based on an analysis of the soil temperature trend under four different treatments, the variation range, variation coefficient and variance in unit soil temperature were calculated. We also analyzed the extent of fluctuation in the unit soil layer of the soil temperature time series and then determined the critical layer of the soil temperature under different snow cover treatments.

Under BL treatment conditions, the variation coefficient of the unit soil layer of soil temperature time series was 12.138% at the 5–10-cm region. As the soil depth increased, the variation coefficient of the unit soil layers gradually decreased, and the fluctuation in the soil temperature sequence gradually weakened. The variation coefficient in soil temperature decreased to 2.645% at the 100–140-cm region. At the same time, the variance of the soil temperature sequence in the unit soil layer was 0.361 °C at the 5–10-cm region; however, the variance of the unit soil layer became 0.061 °C in the 100–140-cm region, wherein the soil temperature deviation from the average value difference gradually decreased. When the soil temperature reached a certain degree of stability, we determined that the soil reached the critical depth.

Under NS conditions, the variation coefficient and variance of the soil temperature in the different soil layers exhibited a decreasing trend compared with those for BL. Among these soil layers, the variation coefficient of the soil temperature at the surface 5–10-cm soil layer was 4.61% lower than that under the BL treatment. At the region below 10 cm, the variation coefficient of the time series gradually decreased, and it was only 1.672% in the 100–140-cm soil layer. The variance of the unit soil layer exhibited similar variation trends from 5 cm to 180 cm.

Similarly, under CS and TS conditions, the variation coefficient and variance in the unit soil temperature were less than those under the BL treatment in the overall change trend; the average values of the soil variation coefficient under the two treatment conditions in the vertical profile decreased by 6.63% and 9.05% compared with those of the BL treatment, and the average values of the variance decreased by 5.43% and 8.69%, respectively. With increasing thickness in snow cover and density, the variation coefficient and variance in soil temperature exhibited a decreasing trend; however, in the 10–15-cm soil layer under the CS treatment and in the 5–10-cm soil layer under the TS treatment, the variation coefficient of soil temperature had a singular value. Based on the results shown in Table 4, the soil variation coefficients (C_v) of the 10–15-cm soil layer under CS conditions and the 5–10-cm soil layer under TS conditions were significantly larger than those of the other soil layers under the same treatment conditions. These results show that the soil temperature of the soil layer is affected by environmental variations; thus, the variation coefficient value is called the singular point. Combined with the experimental conditions, a specific analysis of the reasons for this trend indicated that due to the large amount of snow cover, the infiltration of snowmelt water led to a rapid increase in the soil moisture content. Moreover, as the heat capacity of water of $4.2 \times 10^3 \text{ J}/(\text{kg} \cdot ^\circ\text{C})$ is greater than the soil specific heat [31], a large water supply affected the steady rise of soil temperature [32] and resulted in a certain degree of fluctuation in the soil temperature; thereby, it showed a complex change in the law.

In the process of the research, the difference sequences of the soil temperature between the 10, 15, 20, 40, 60, 100, 140 and 180-cm layers and the surface 5-cm layer were calculated. On this basis, the variances of the difference sequences were obtained. As the variance reflects the degree of discretization of the sequence, it also reflects the stability of the sequence. The temperature sequence of the 5-cm soil layer had a greater degree of fluctuation, so we believed that the research soil layer had a strong degree of dispersion when the variance of the difference sequence between the research soil layer and the 5-cm soil layer was small. When the variance of the difference sequence increased and tended to a stable value, the temperature of the research soil layer reached a stable state.

Figure 6 shows that the variance curves in the soil temperature difference under the four different treatments had a “steady-rising-steady” trend. As the changing tendency of the soil temperature at the 10, 15 and 20-cm soil layers was similar to that of the surface 5-cm soil layer, the variance of the difference sequence between these soil layers and the 5-cm soil layer was low. With the increase in soil depth, the variances of the difference sequence between the 100, 140 and 180-cm soil layers and the surface 5-cm soil layer were larger and tended to a steady state. This indicated that the temperatures of the 100, 140 and 180-cm soil layers were different from that of the surface 5-cm layer. The soil temperatures of these soil layers were relatively stable and did not fluctuate. Therefore, it seemed that when the variance curve approached a plateau, the soil temperature tended to stabilize and become less affected by the fluctuation of freezing and thawing.

In the study, the curve in the figure was fitted by the variance values of the nine difference sequences, and the variation process of the variance under the different treatment conditions conformed to the logistic curves. Through the analysis by fitting toolbox in MATLAB (Matlab software v. 2010b, MathWorks, Natick, MA, USA), we can see that the determination coefficient (R^2) was 0.993 under the condition of bare land; the fitting degree of the curve was higher; and the specific equation of the curve was $y = 25.12/[1 + 0.594e^{-0.0534(x-90)}]$. Besides that, the determination coefficients were 0.987, 0.952 and 0.931 under the condition of NS, CS and TS, respectively. We think that the location where the curve tended to be stable was the critical layer of the soil freezing and thawing activities. In order to

seek the critical point, the first derivative of the curve equation was calculated by MATLAB software, and we defined that when the first derivative of the equation was less than 0.1, the slope of the curve tends to be stable and that was the critical layer of soil water thermal activity. By comparison, we can see that the critical layer under BL conditions was 124 cm, and the critical positions under NS, CS and TS conditions were 112, 97 and 88 cm, respectively. The error between the soil frozen depth and the critical layer depth remained within 5%, which was consistent with the actual situation.

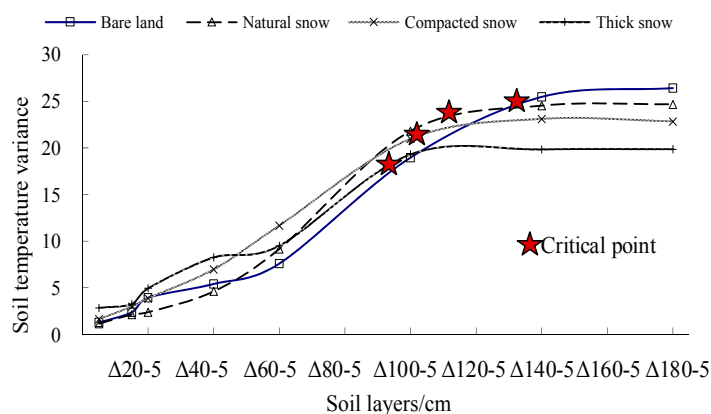


Figure 6. Variation in the soil temperature variance.

3.3. Variation in Soil Moisture Content

This change in soil moisture content during the freezing and thawing period is shown in Figure 7. In the BL treatment, the variation difference in the soil moisture content was 28.76% in the 0–40-cm soil layer. With the increasing depth of the soil layer, the variation difference of the soil water content became 20.03% in the 40–140-cm soil layer, and there was still a considerable difference in the variation of the water content. However, in the deep 140–180-cm layer, the soil moisture content was essentially stable, and the difference in moisture content was only 3.7%, whereas the decrease in soil water content was primarily due to the migration of soil moisture to the frozen edge.

Under NS conditions, the overall level of soil moisture content was higher than in the BL treatment, and the variation difference also exhibited a certain degree of reduction. The difference in the soil moisture content was 23.45% in the 0–40-cm soil layer, and it decreased by 5.31% compared with that for the BL treatment. In the 40–140-cm and 140–180-cm soil layers, the difference in soil moisture content decreased by 6.14% and 1.32% compared to the BL treatment, respectively. The snow cover treatment reduced the soil heat dissipation, and the freeze degree of soil decreased, which led to a decrease in the soil moisture content.

Under CS and TS, because of the increase in the thickness of the snow cover and the snow density, the effects of heat preservation and water conservation were more obvious. The differences in the soil moisture content in the 0–40-cm soil layer under the two treatments were 6.31% and 7.26% lower than those under the BL treatment, respectively. Furthermore, in the 40–140-cm and 140–180-cm soil layers, the variation difference of the soil moisture content exhibited a certain degree of reduction compared to that in the BL treatment, and the overall level of the soil moisture content exhibited an increasing trend.

We also analyzed the range, variation coefficient and variance of the soil moisture content per unit soil layer under the four different snow cover treatments, and the results are shown in Table 5.

Under the BL treatment conditions, the variation coefficient of the soil moisture content in a unit soil layer was 12.634% at the 5–10-cm soil layer. The variation coefficient of the soil moisture content vertical profile showed a trend of gradually narrowing from shallow to deep until reaching

the 100–140-cm soil layer, wherein its variation coefficient decreased to 0.964%, and the soil moisture content reached a relatively stable level.

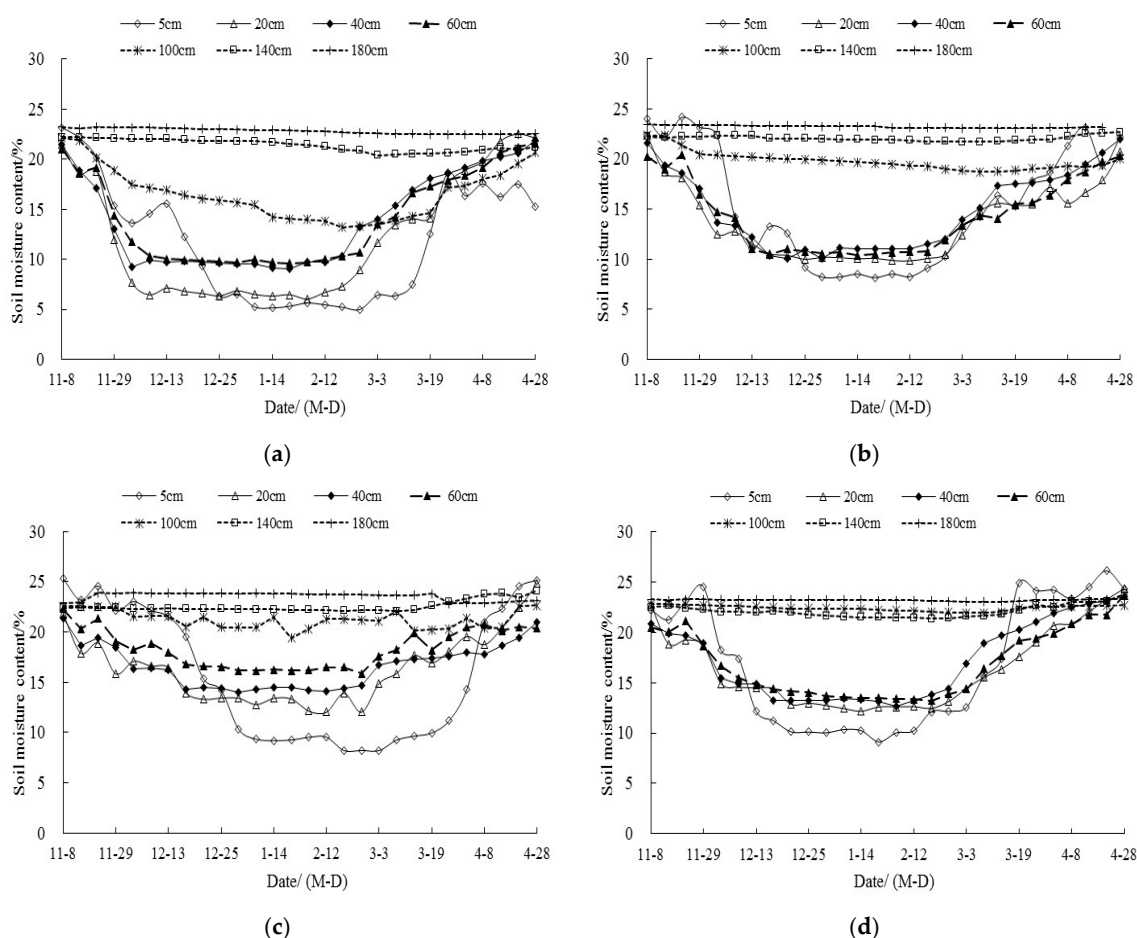


Figure 7. Variation in soil water content under different snow cover treatments. (a) Bare land; (b) natural snow; (c) compacted snow; (d) thick snow.

Table 5. Analysis of soil water content variability in unit soil layers under different snow cover treatments.

Soil Depth (cm)	Bare Land			Natural Snow			Compacted Snow			Thick Snow		
	R (%)	C _v (%)	D (%)	R (%)	C _v (%)	D (%)	R (%)	C _v (%)	D (%)	R (%)	C _v (%)	D (%)
Δ(10–5)/5	2.39	12.634	1.263	2.37	8.345	1.387	2.54	9.046	1.164	2.92	12.241	1.441
Δ(15–10)/5	1.66	8.614	1.187	2.08	11.234	1.274	3.15	10.895	1.442	3.68	9.342	1.017
Δ(20–15)/5	1.77	5.431	0.952	1.62	6.534	0.986	4.05	6.734	0.948	4.69	6.345	0.814
Δ(40–20)/20	0.60	4.214	0.723	0.47	4.537	0.787	0.59	3.279	0.568	1.12	5.435	0.517
Δ(60–40)/20	0.35	2.217	0.692	0.53	2.298	0.718	0.72	2.975	0.507	0.80	2.178	0.529
Δ(100–60)/40	0.28	1.136	0.401	0.47	1.796	0.527	0.42	1.379	0.396	0.44	1.375	0.384
Δ(140–100)/40	0.20	0.964	0.363	0.19	0.867	0.460	0.33	1.124	0.247	0.35	0.768	0.254
Δ(180–140)/40	0.11	0.274	0.121	0.20	0.386	0.143	0.31	0.375	0.130	0.18	0.274	0.127

Notes: R represents the range; C_v represents the coefficient of variation; D represents the variance.

Under the NS conditions, the variation coefficient of the soil moisture content in the shallow soil also exhibited a high level of variability; however, the variation in the vertical profile indicated that the variation coefficient of the soil moisture content in a unit soil layer was 8.345% in the 5–10-cm soil layer. Furthermore, the variation coefficient reached a peak value in the 10–15-cm soil layer. The area below

this soil layer indicated a trend of decreasing gradually, then tending to be stable in the 100–140-cm soil layer. An analysis indicated that the infiltration of snowmelt water in the spring resulted in a sudden increase in soil moisture content at the soil surface, which affected the whole process of soil moisture content; therefore, the coefficient of variation in the soil layer also had a certain impact.

Similarly, under the CS and TS treatments, the variation coefficient of soil moisture content exhibited a peak at 10–15 cm and 5–10 cm, respectively. With an increasing amount of snow cover, the infiltration of the snowmelt water increased, and the variation coefficient of the liquid water content in the peak level position gradually rose. However, the variation coefficient of the soil moisture content in the vertical sections of soil also tended to decrease with the increasing soil depth.

We sought to determine the difference in the soil moisture content between each layer and the surface 5-cm layer in the four different treatments and calculated the variance of the difference. The results are shown in Figure 8.

Comparing the variances of the difference sequences in the soil moisture content under the four different treatment conditions revealed that the soil variation trend was gentler in the shallow soil. After the rising stage, the soil moisture content of the soil under the TS treatment was the first to reach a stable level, and the inflection point was at 89 cm. Then, the variance of the difference sequence of the moisture content reached an equilibrium under the CS treatment, and the inflection point was located in the 98-cm soil layer. The CS, NS and BL treatments reached their equilibrium positions in that order; the variance balance value decreased with the increasing snow cover, and the critical layer of the soil water heat activity gradually decreased.

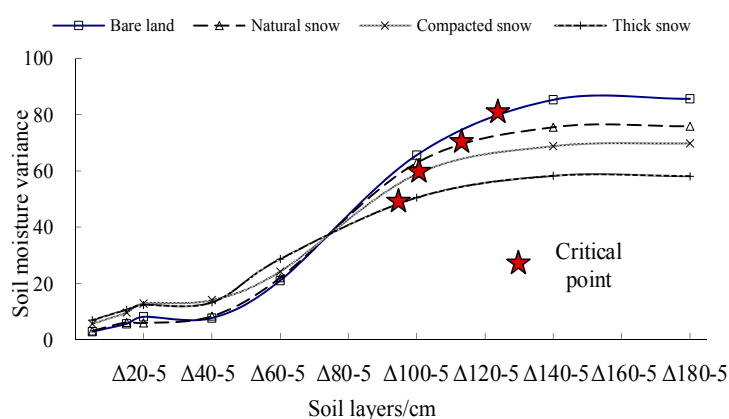


Figure 8. Variation in soil water content.

In summary, the changes in the soil moisture content in the shallow soil layers were relatively drastic, whereas those in the deeper soil layers were relatively stable. Snow cover can reduce the evaporation and diffusion of soil moisture, thereby reducing water loss, whereas the effect of snow insulation lessened the degree of soil freezing and increased the overall moisture content of the soil. The difference in soil moisture content gradually decreased with the increasing snow thickness and density.

4. Discussion

(1) The results of this paper were based on measured data. By analyzing the changes in the soil freezing rate, soil temperature and water content, the stable level of the soil water and heat change was found, which was defined as the critical layer of soil freezing and thawing. The differences in the soil freezing and thawing critical layer positions under different snow cover conditions were compared, and the influence of meteorological factors on the soil water and heat transfer activities were analyzed. However, the physical response mechanism of the atmospheric-soil complex system and its quantitative transfer relationship require further study.

(2) Under the driving force of the soil matric potential, the frozen front of the soil moved deeper during the process of soil freezing. It can be seen from the analysis that in the 10–60-cm soil layer, the soil freezing rate was greater, and the surface soil was more affected by the environmental variation. In the 90–130-cm soil layer, the soil freezing rate was slow, and with the increase in soil depth, the energy exchange between the soil and the environment was attenuated. Wang [33] proposed that the heat flux decreased in the deep soil, and with the passage of time and the increase in the freezing depth, the freezing rate became slow. From the analysis of the article, we also can see that the level of soil freezing stability under the condition of snow cover increased by nearly 10 cm compared with that of bare land, and the position of the frozen layer of the soil increased in turn under the natural snow, compacted snow and thick snow cover treatment conditions. Calonne [34] proposed that the low thermal conductivity and high heat capacity of the snow weakened the heat transfer between the soil and the environment. Guo [35] also suggested that the snow cover hindered the effect of the solar radiation on the soil temperature, reduced the diffusion of the soil heat and narrowed the freezing range of the soil. This study confirmed the effect of snow cover on the location of the soil critical layer.

(3) With the decreasing ambient temperature, the soil temperature fluctuated to different degrees due to the influence of the environment. The soil water and heat conditions of the different soil layers are quite different. With the increasing soil depth, heat transfer was accompanied by a phenomenon of dissipation, and the soil thermal conductivity was weakened. The results showed that the change trend of the soil temperature in the 0–40-cm region was significantly larger than that of the 140–180-cm region, and combined with the temperature range, variation coefficient and variance of the unit soil layer, the soil temperature fluctuated significantly in the 0–40-cm area, but it tended to be stable in the 140–180-cm region. Li [36] proposed that during the freezing-thawing cycle of frozen soil, with the increase in soil depth, the amplitude of the soil change decreased, and the freezing time was thus delayed. Liu [37] considered that the temperature of the surface area changes significantly in the process of water circulation between the ground gases, while in the area below 65 cm, the soil energy region was stable. At the same time, the research showed that the strong emissivity and low thermal conductivity hindered the energy exchange between the soil and the environment, so the range of the soil temperature variation narrowed with the increasing snow cover.

(4) During the freezing process, under the action of a temperature gradient, the soil moisture changed from the liquid phase to the solid phase and migrated under a driving force. In the melting period, with the increase in the ambient temperature, the solid ice in the soil was converted into liquid water, and the infiltration of the snow melt also supplied surface soil moisture. It was found that the soil water content in the 0–40-cm soil layer decreased significantly during the freezing period, while the water content of the melting period increased significantly, and the variation range was higher than that of the melting period in the 40–140-cm and 140–180-cm soil areas. It is believed that the energy was lost in the transmission during the freezing process, and the phase change of the solid ice absorbed a substantial amount of this energy; it hindered the process of energy transfer from the shallower to the deeper, and thus, the response of the soil moisture to the surface environment decreased with the depth of the soil. Fan [38] proposed that the water contents of the different soil layers showed a “U” trend in the process of the freeze-thaw cycle, and the driving effect of the temperature gradient weakened with the increasing soil depth. In addition, evaporation of the soil water was inhibited by the snow cover, and the degree of soil freezing was weakened by the snow insulation effect. With the increase in the snow cover thickness and the increase in density, this effect was more significant.

5. Conclusions

(1) Snow is a poor conductor of heat, and it reduced the energy exchange between the environment and the soil in the atmosphere-snow-soil complex; in addition, it hindered the two-way transmission of heat, which affected the migration rate of the frozen front during the freezing process. Therefore, the snow decreased the freezing depth of the soil and prolonged the soil melting time. The average soil freezing rates under natural snow, compacted snow and thick snow treatments decreased by 8.29%,

12.32% and 25.87% compared with a bare land treatment, respectively. With increasing thickness of the snow cover and increasing density, the barrier between the soil and the environment was enhanced, and the frozen area of soil decreased.

(2) During the freezing and thawing cycles, the strong reflectivity of the snow and the large heat capacity suppressed the influence of atmospheric radiation and environmental vapor pressure driving soil water and heat. In the process of vertical and horizontal water and heat transfer, the variation in soil temperature in the shallow soil layer was relatively large, but at a depth of 140 cm, the difference in the soil temperature and time series was very weak. The insulating effect was more obvious at shallower soil depths. With each freezing phase, the soil surface soil moisture content significantly decreased. During the melting period, the infiltration of the snow melt water caused a sudden increase in the shallow water content, and the change in the soil moisture content in the shallow soil layer was relatively complicated. The trend in deep-water content was a gradual decrease.

(3) The variation in the soil temperature and liquid water content difference at each soil layer with changes in soil surface water and heat time series defined the position of the soil critical layer. The results were in strong agreement with the results of a soil freezing depth analysis and per unit of soil moisture variability. It was further verified that the existence of snow reduces the influence of the atmospheric environment on soil water-heat transfer. The snow cover weakened the influence of temperature on soil water and heat. With increasing snow cover, the critical layer of soil freeze and thaw gradually increased.

(4) These results can provide a basis for the determination of the critical level of soil water and heat activity in regions with seasonally frozen soil. Defining the active range of the freezing and thawing soil water heat ensures that researchers can study the migration mechanisms and the coupling relationships between the soil and water, improving the authenticity and reliability of theoretical research. In addition, this study has important guiding significance for predicting the spatial distribution of soil water and heat in the active layer, thereby providing timely support for scientific and reasonable formulations of the spring sowing plan.

Acknowledgments: This research was supported by National Natural Science Foundation of China (51679039), the Heilongjiang Province Changjiang Scholar Reserve Support Project and the Outstanding Youth Fund of Heilongjiang Province (JC201402).

Author Contributions: Qiang Fu and Renjie Hou designed the study. Qiang Fu and Renjie Hou wrote the manuscript. Renjie Hou and Tianxiao Li performed the data analysis. Renjie Hou, Peiru Yan and Ziao Ma reviewed and approved the manuscript.

Conflicts of Interest: The authors declare no conflicts of interest.

References

1. Wang, Y.; Liu, J.S.; Wang, G.P. Study on the effect of freezing and thawing action on soil physical and chemical characteristics. *Geogr. Geo-Inf. Sci.* **2007**, *23*, 91–96.
2. Larsen, K.S.; Jonasson, S.; Michelsen, A. Repeated freeze–thaw cycles and their effects on biological processes in two arctic ecosystem types. *Appl. Soil Ecol.* **2002**, *21*, 187–195. [[CrossRef](#)]
3. Potter, C. Predicting climate change effects on vegetation, soil thermal dynamics, and carbon cycling in ecosystems of interior Alaska. *Ecol. Model.* **2004**, *175*, 1–24. [[CrossRef](#)]
4. Wu, Z.F.; Jin, Y.H.; Liu, J.P. Response of vegetation distribution to global climate change in Northeast China. *Sci. Geogr. Sin.* **2003**, *23*, 564–570.
5. Zhang, X.L.; Zhou, Z.M.; Liu, J.L. Melting of seasonal snow cover and its influence on soil temperature conditions of shallow layer. *Trans. CSAE* **2010**, *26*, 91–95.
6. Tian, H.; Wei, C.; Wei, H. Freezing and thawing characteristics of frozen soils: Bound water content and hysteresis phenomenon. *Cold Reg. Sci. Technol.* **2014**, *103*, 4–81. [[CrossRef](#)]
7. Li, R.P.; Shi, H.B.; Takco, A. Study on water-heat-salt transfer in soil freezing-thawing based on simultaneous heat and water model. *J. Hydraul. Eng.* **2009**, *40*, 403–412.
8. Hui, B.; Ping, H.; Ying, Z. Cyclic freeze–thaw as a mechanism for water and salt migration in soil. *Environ. Earth Sci.* **2015**, *74*, 675–681.

9. Li, R.P.; Shi, H.B.; Takeo, A. Characteristics of air temperature and water-salt transfer during freezing and thawing period. *Trans. CSAE* **2007**, *23*, 70–74.
10. Korolyuk, T.V. Specific features of the dynamics of salts in salt-affected soils subjected to long-term seasonal freezing in the south Transbaikal region. *Eurasian Soil Sci.* **2014**, *47*, 339–352. [[CrossRef](#)]
11. Urakawa, R.; Shibata, H.; Kuroiwa, M. Effects of freeze–thaw cycles resulting from winter climate change on soil nitrogen cycling in ten temperate forest ecosystems throughout the Japanese archipelago. *Soil Biol. Biochem.* **2014**, *74*, 82–94. [[CrossRef](#)]
12. He, H.; Dyck, M.F.; Si, B.C. Soil Freezing–Thawing Characteristics and Snowmelt Infiltration in Cryalfts of Alberta, Canada. *Geoderma Reg.* **2015**, *5*, 393–405. [[CrossRef](#)]
13. Zollinger, B.; Alewell, C.; Kneisel, C. Effect of permafrost on the formation of soil organic carbon pools and their physical–chemical properties in the Eastern Swiss Alps. *Catena* **2013**, *110*, 70–85. [[CrossRef](#)]
14. Musa, A.; Liu, Y.; Wang, A. Characteristics of soil freeze–thaw cycles and their effects on water enrichment in the rhizosphere. *Geoderma* **2016**, *264*, 132–139. [[CrossRef](#)]
15. Flerchinger, G.N.; Lehrsch, G.A.; McCool, D.K. Freezing and thawing processes. In *Encyclopedia of Soils in the Environment*; Elsevier: Oxford, UK, 2005; pp. 104–110.
16. Iwata, Y.; Nemoto, M.; Hasegawa, S. Influence of rain, air temperature, and snow cover on subsequent spring-snowmelt infiltration into thin frozen soil layer in northern Japan. *J. Hydrol.* **2011**, *401*, 165–176. [[CrossRef](#)]
17. Chen, H.S.; Sun, Z.B. Design of a comprehensive land surface model and its validation part I. model description. *Chin. J. Atmos. Sci.* **2004**, *6*, 801–819.
18. Bonnaventure, P.P.; Lewkowicz, A.G.; Kremer, M. A Permafrost Probability Model for the Southern Yukon and Northern British Columbia, Canada. *Permafr. Periglac. Process.* **2012**, *23*, 52–68. [[CrossRef](#)]
19. Kurylyk, B.L.; Mckenzie, J.M.; Macquarrie, K.T.B. Analytical solutions for benchmarking cold regions subsurface water flow and energy transport models: One-dimensional soil thaw with conduction and advection. *Adv. Water Res.* **2014**, *70*, 172–184. [[CrossRef](#)]
20. Xiang, X.H.; Wu, X.L.; Wang, C.H. Influences of climate variation on thawing–freezing processes in the northeast of Three-River Source Region China. *Cold Reg. Sci. Technol.* **2013**, *86*, 86–97. [[CrossRef](#)]
21. Yang, M.; Yao, T.; Gou, X. The soil moisture distribution, thawing–freezing processes and their effects on the seasonal transition on the Qinghai–Xizang (Tibetan) Plateau. *J. Asian Earth Sci.* **2003**, *21*, 457–465. [[CrossRef](#)]
22. Nelson, F.E.; Anisimov, O.A.; Shiklomanov, N.I. Subsidence risk from thawing permafrost. *Nature* **2001**, *410*, 889–890. [[CrossRef](#)] [[PubMed](#)]
23. Ge, S.; Wu, Q.B.; Lu, N. Groundwater in the Tibet Plateau, western China. *Geophys. Res. Lett.* **2008**, *35*, 80–86. [[CrossRef](#)]
24. Ge, S.; Mckenzie, J.; Voss, C. Exchange of groundwater and surface-water mediated by permafrost response to seasonal and long term air temperature variation. *Geophys. Res. Lett.* **2011**, *38*, 3138–3142. [[CrossRef](#)]
25. Shiklomanov, D.N.I.; Nelson, F.E. Active-layer mapping at regional scales: A 13-year spatial time series for the Kuparuk region, north-central Alaska. *Permafr. Periglac. Process.* **2002**, *13*, 219–230. [[CrossRef](#)]
26. Liu, W.H.; Xie, C.W.; Zhao, L. Simulating the active layer depth and analyzing its influence factors in permafrost of the Mahan Mountain, Lanzhou. *J. Glaciol. Geocryol.* **2015**, *37*, 1443–1452.
27. Zhang, W.; Zhou, J.; Wang, G.X. Monitoring and modeling the influence of snow cover and organic soil on the active layer of permafrost on the Tibetan Plateau. *J. Glaciol. Geocryol.* **2013**, *35*, 528–540.
28. Chang, J.; Wang, G.X.; Li, C.J. Seasonal dynamics of suprapermafrost groundwater and its response to the freeing–thawing processes of soil in the permafrost region of Qinghai–Tibet Plateau. *Sci. China Earth Sci.* **2015**, *45*, 481–493. [[CrossRef](#)]
29. Xing, X.G.; Zhao, W.G.; Ma, X.Y. Temporal stability of soil salinity in root zone of cotton under drip irrigation with plastic mulch. *Trans. Chin. Soc. Agric. Mach.* **2015**, *46*, 146–153.
30. Wang, W.H.; Wang, Q.J. Scale-dependency of spatial variability of soil Air permeability on typical oasis croplands at middle reaches of Heihe river. *Trans. Chin. Soc. Agric. Mach.* **2014**, *45*, 179–183.
31. Xiao, X.; Liu, G.; Li, B.G. Finite element analysis of effect of soil pores on measurement of specific heat with the Dual-Probe Heat-Pulse method. *Acta Pedol. Sin.* **2013**, *50*, 1138–1142.
32. Fu, Q.; Hou, R.J.; Wang, Z.L. Soil moisture thermal interaction effects under snow cover during freezing and thawing period. *Trans. CSAE* **2015**, *31*, 101–107.

33. Wang, E.L.; Zhang, A.Q.; Bao, T.E. Variability analysis of freezing depth mode of vertical buried pipes with different materials in cold area. *J. Hydraul. Eng.* **2017**, *48*, 86–95.
34. Calonne, N.; Flin, F.; Morin, S. Numerical and experimental investigations of the effective thermal conductivity of snow. *Geophys. Res. Lett.* **2011**, *38*, 537–545. [[CrossRef](#)]
35. Guo, L.P.; Li, L.H.; Xu, J.R. Responses of snow depth and seasonal frozen ground temperature to enhanced air temperature in Kunges Valley, Tianshan Mountains. *Res. Sci.* **2012**, *34*, 636–643.
36. Li, W.P.; Fan, J.H.; Sha, Y.K. Soil Temperature Variation and Thaw-freezing Cycle in the Alpine Cold Steppe, Northern Tibetan Plateau. *J. Mt. Sci.* **2014**, *32*, 407–416.
37. Liu, G.S.; Wang, G.X.; Sun, X.Y. The response of soil moisture in swamp meadow in the source regions of the Yangtze River to artificially warming. *J. Glaciol. Geocryol.* **2015**, *37*, 668–675.
38. Fan, J.H.; Lu, D.Y.; Wang, X.D. The freezing-thawing processes and soil moisture-energy distribution in permafrost active layer, Northern Tibet. *J. Mt. Sci.* **2014**, *32*, 385–392.



© 2017 by the authors. Licensee MDPI, Basel, Switzerland. This article is an open access article distributed under the terms and conditions of the Creative Commons Attribution (CC BY) license (<http://creativecommons.org/licenses/by/4.0/>).